RGNZ/MGPB

Rudarsko-geološko-naftni zbornik
(The Mining-Geology-Petroleum Engineering Bulletin)
DOI: 10.17794/rgn.2026.3.9

Original scientific paper

Geochemistry and genesis of the manganese ores in the Nawagai ophiolitic melange, Mohmand District, Khyber Pakhtunkhwa, Pakistan

Irfan Ullah[1], **Aamir Khan**[2,3,1*], **Mohammad Tahir Shah**[1], **Liaqat Ali**[1*], **Asad Khan**[4,5], **Muhammad Mustafa**[6]

[1] *National Center of Excellence in Geology, University of Peshawar, Peshawar 25130, Pakistan.*
[2] *State Key Laboratory for Critical Mineral Research and Exploration, Institute of Geochemistry, Chinese Academy of Sciences, Guiyang 550081, China.*
[3] *University of Chinese Academy of Sciences, Beijing, 100049, China.*
[4] *Department of Earth Sciences, FATA University, FR Kohat 26100, Pakistan.*
[5] *State Key Laboratory of Critical Mineral Research and Exploration, School of Geosciences and Info-Physics, Central South University, Changsha 410083, China.*
[6] *College of Geosciences, China University of Petroleum (Beijing), Beijing 102249, China.*

Abstract

The Nawagai ophiolitic melange is present in the western part of the Main Mantle Thrust /Indus Suture Zone (MMT/ISZ) in northern Pakistan and is considered as a part of the fold belt that contains ophiolitic sequences. The studied manganese ore bodies are present in the Nawagai ophiolitic melange in the Mohmand District of Khyber Pakhtunkhwa, Pakistan. These ores are dislocated lenticular bodies of various size and are generally associated with the cryptocrystalline meta-chert. Both Mn-ores and the host meta-cherts are highly tectonized and are, therefore, subjected to metamorphism/deformation. Mineralogically, the studied Mn-ores are dominantly composed of braunite with a lesser amount of pyrolusite and piemontite as Mn-bearing phases while the gangue minerals are mainly cryptocrystalline quartz with a lesser amount of calcite. The Mn-phases are interlocked within the cryptocrystalline quartz; however, the cross cutting micro-veins of quartz and calcite are also noticed. At places the pyrolusite and piemontite are replacing braunite. Geochemically, the studied Mn-ores are highly variable in their grade. These are generally high-grade to low-grade but as a whole, from an economic perspective, these ores can be considered as low-grade ores on the basis of MnO, Fe_2O_3 and SiO_2 contents. No correlation among the major elements has been found, however, significant positive correlation between SiO_2 and MnO has been noted. The fractionation behaviour of Mn and Fe and the concentration of various major and trace elements suggest that the studied Mohmand area Mn-ores have been formed from the hydrothermal fluid distal to the source (vent) with the input from the pelagic sediments along the mid-ocean ridges within the Neo-Tethys Ocean. These have been obducted, as exotic bodies within ophiolitic sequences, on the Indian Plate due to the subduction of Indian Plate underneath the Kohistan Island Arc along the MMT/ISZ. These Mn-ores and the meta-cherts have attained severe metamorphism and deformation during and after the emplacement of the ophiolitic bodies in the existing position.

Keywords:
manganese, petrography, mineralogy, geochemistry, ore genesis

1. Introduction

Manganese is a key element of the ferroalloy metals which is mainly used in steel making, and other metallurgical, battery and chemical industries. It is mostly used in the form of ferromanganese (FeMn) and silicomanganese (SiMn) and various compounds such as $MnSO_4$, $MnCl_2$, KMn, etc. in various industries. In the steel industry, it is used for the removal of oxygen and sulfur, which imparts hardness, malleability, and tenacity to steel. Steel made of ferromanganese and silicomanganese is used in construction and transportation machinery (**Siddiquie et al. 2015; Rehman et al. 2020**). The chemical grade of Mn is used in the production of chemicals, batteries, glass, plant food, paints, and pigments, as well as in the textile industry. It is also used as a water purifier, catalyst and as a carrier of oxygen for chemical looping combustion (CLC) (**Mehdilo and Irannajad 2014; Haider et al. 2016**). Globally, most of the Mn (90-95%) produced annually (with Mn content greater than 40 %) is used in the steel industry as a deoxidizer and desulfurizer. The remaining (5-10%) is

* Corresponding author: Aamir Khan
e-mail address: aamir-khan@mail.gyig.ac.cn
Received: 14 August 2025. Accepted: 2 December 2025.
Available online: 14 May 2026

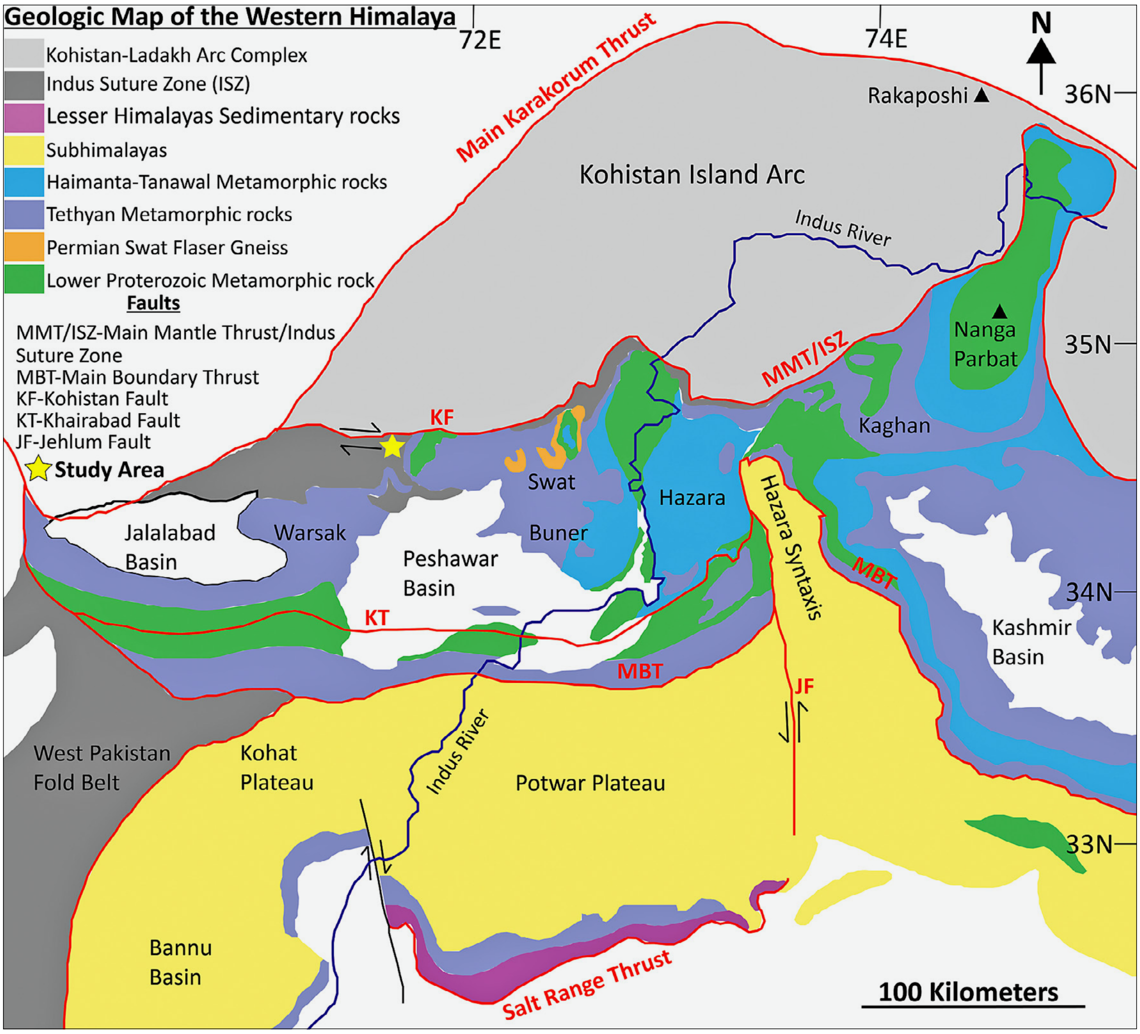

Figure 1. Geotectonic map of northern Pakistan showing the location of the study area (after **DiPietro and Pogue 2004**)

consumed by other sectors, such as the chemical, paint, fertilizer, batteries and glass industries (**Lasheen et al. 2009**).

World over, Mn-deposits have been formed in various tectonic settings which include continental sedimentary sequences, as well as ophiolites. These deposits can be divided into three broad categories (1) hydrothermal (2) hydrogenous and (3) digenetic/biogenetic-bacterial deposits (**Polgári et al. 2012; Öksüz 2011**). Hydrothermal deposits form through direct precipitation from hydrothermal solutions at low temperatures (**Hein et al. 1997; Ingram et al. 1990**). These deposits are typically strata bound and laminated or can exist as irregular bodies and epithermal veins. They are discovered in both present-day and past marine environments, located near spreading centers or intraplate seamounts, as well as in island arc settings associated with subduction (**Polgári et al. 2012; Baba et al. 2003; Öksüz and Okuyucu 2014**). Hydrogenous deposits are composed of ferromanganese crusts, which are rich in amorphous iron compounds and usually depleted in Mn minerals. It slowly precipitates from seawater from microbial activity at rates of 2 to 10 mm per Ma on the seafloor (**Öksüz 2011; Jach and Dudek 2005; Toth 1980**). Hydrogenous deposits are characterized by high trace element concentrations, particularly Ni and Cu and a low Mn/Fe ratio (~1) (**Hein et al. 1997, 1996; Usui and Someya 1997; Usui and Nishimura 1992; Ingram et al. 1990; Toth 1980**). Diagenetic/biogenetic-bacterial manganese deposits are formed in nodules and precipitate with the effect of hydrothermal solutions in the form of Mn-carbonate mineralization due to oxidation of organic matter (**Polgári 1991; Polgári et al. 2012; Öksüz 2011**). Although the hydrothermal and diagenetic deposits are characterized by high Mn/Fe ratios and low trace metal contents (**Hein et al. 1996, 2013**) but these can be distinguished on the basis of their morphology, tectonic setting and growth rates (**Kuhn et al. 1998**; **Choukrad et al. 2022**).

In Pakistan, low to medium-grade Mn-deposits, associated with a continental sedimentary sequence, are reported in Chura Gali, Galdanian and Kakul from the Hazara region of Khyber Pakhtunkhwa Province, (**Shah and Moon 2004, 2007**). Similarly, Mn deposits that are associated with ophiolitic rocks are reported from North

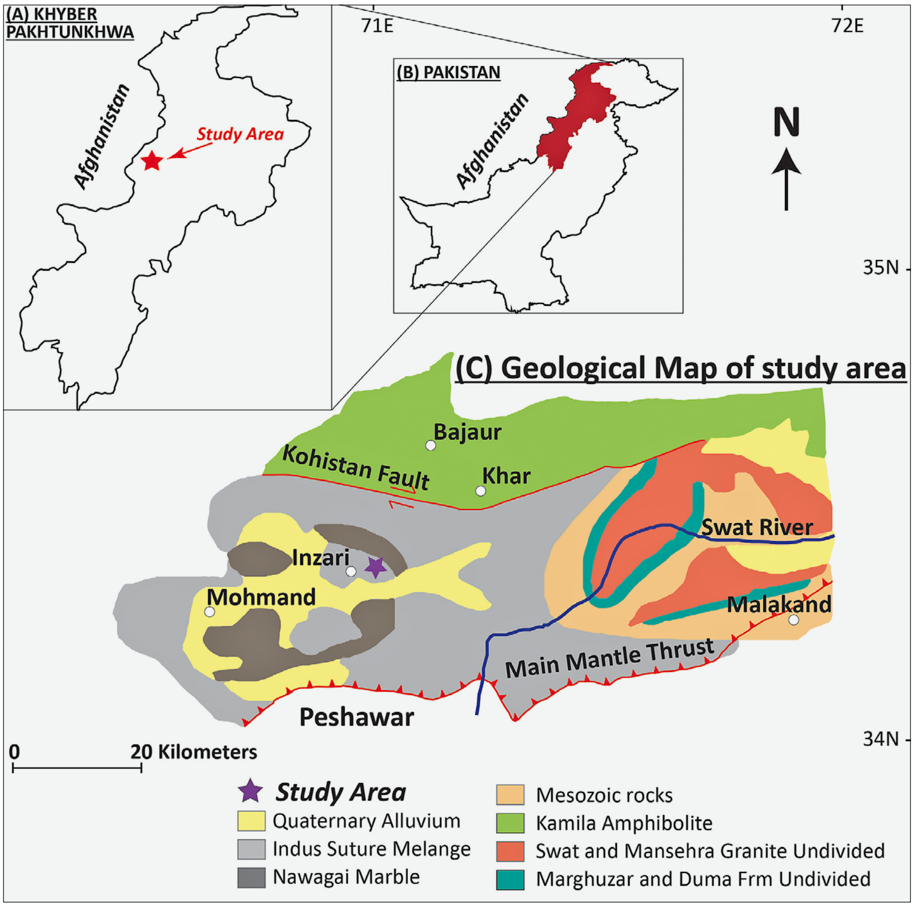

Figure 2. Geological map of the Mohmand District taken and modified from **Aslam et al. (2006)**, showing the location of the study area.

Waziristan (**Shah and Khan 1999; Shah and Moon 2007**), Lasbela-Khuzdar, Zhob (**Naseem et al. 1997; Khan et al. 2020**) and the Bela area (**Narijo et al. 2019**).

2. Regional Geology

Northern Pakistan has two major regional-scale tectonic faults, namely the Main Mantle Thrust (MMT) / Indus Suture Zone (ISZ) in the south and the Main Karakorum Thrust (MKT) in the north (see **Figure 1**). These two thrust faults have geologically divided northern Pakistan into three separate tectonic domains from north to south, i.e. Karakoram block (KB), the Kohistan Island Arc (KIA) and the Indian Plate (IP) (see **Figure 1**) (**Tahirkheli 1979; Bard 1983; Treloar 1989; Khan et al. 1993; Burg 1996; Kazmi and Jan 1997; Searle et al. 1999**). The MMT/ISZ defines the tectonic boundary between the KIA and the IP in the south. During the Paleogene, it developed as a result of the closing of the Neo-Tethys Ocean and eventual collision of the northern Indian Plate edge with the Kohistan and Ladakh Arc (**Molnar and Tapponnier 1975; Tahirkheli 1979; Klootwijk et al. 1992**). The MMT/ISZ is not a single fault but a sequence of faults with varying ages and tectonic histories (**Searle et al. 1999; DiPietro et al. 2000**). A thick zone of sheared ophiolitic melanges appears along the MMT/ISZ (see **Figure 1**). From east to west along the MMT/ISZ, these are the Mingora, Charbagh and Shangla ophiolitic melange zone, Malakand and Dargai ophiolitic melanges and the Nawagai ophiolitic melange (**Kazmi et al. 1984; DiPietro et al. 1991; 2008**). These ophilitic melanges are characterized by a variety of highly deformed ophiolitic rocks that have undergone varying degrees of metamorphism (**Kazmi and Jan 1997; Ahmad and Jehan 2006**). Serpentinite, dunite, lherzolite, gabbro, basalt, and sedimentary rocks like limestone and chert (pelagic sediments) are the predominant rocks of these melange zones. These rocks have undergone varying degrees of mixing and metamorphism as a result of the numerous tectonic processes that occurred during the development of the suture zone (**Robertson 2000**). These melanges also contain a range of valuable metallic and non-metallic mineralization including chromite, manganese, platinum group elements (PGEs), nickel, emerald and nephrite, etc. (**Ahmad and Jehan 2006**).

2.1. *Geology of Study Area*

The study area lies in the Toposheet No. 38N/06 of the Geologic Survey of Pakistan. It is located in the vicinity of Inzari Village in the Mohmand District which is easily accessible from Peshawar, the capital city and a district of Khyber Pakhtunkhwa (KP) Province (see **Figure 2**). The Mohmand District shares its borders with the Bajaur District in the north, the Khyber District in the

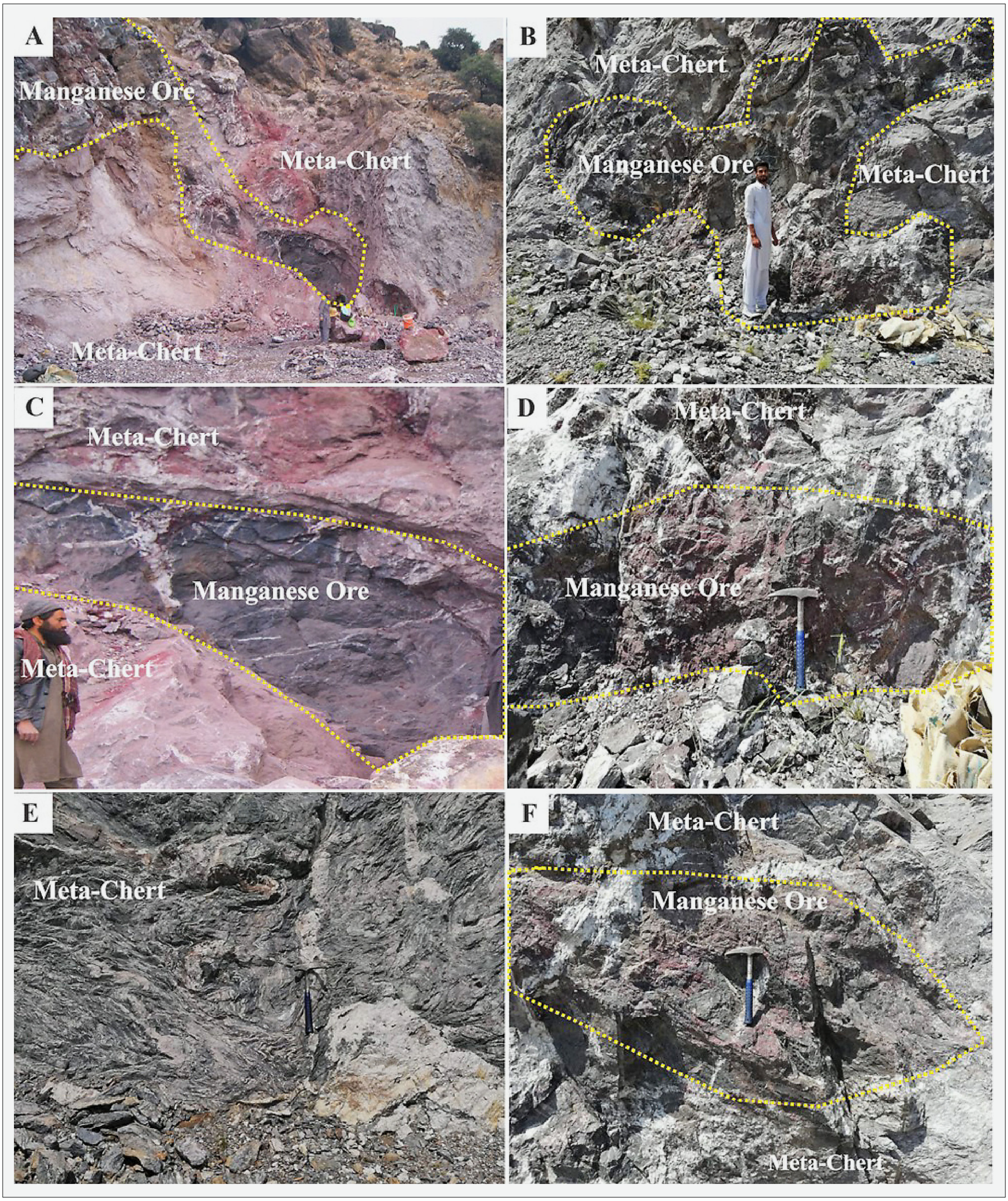

Figure 3. Field photographs of manganese ores: (A & B) tectonized bodies of manganese enclosed in the host rock (meta-chert), (C) Manganese ores are cross-cut by quartz and calcite veins, (D) Hand specimen showing pull apart texture where fractures are filled with quartz and carbonates, (E) Intense shearing and foliation in shear zones, (F) Lensed shaped manganese ore enveloped by host rock.

south, Malakand and Charsadda districts in the east and the Peshawar District in the southeast. Geologically, the study area is located in the Nawagai ophiolitic melange (**DiPietro et al. 1991; 2008**), which is a part of the Indus suture melange and is lying in the western most part of the MMT/ISZ (**DiPietro and Pogue 2004**). The dominant lithologies of the Nawagai ophiolitic melange are marble, dunite, serpentinite, greenstone, grey to black and green phyllites while talc-carbonate schist occurs as a subordinate lithology (**Aslam et al. 2006**). Cryptocrystalline meta-chert showing grey to reddish-brown colouration, along with clay minerals and at places marble is hosting the Mn mineralization in the Mohmand area (see **Figure 3**). The manganese ores are identified by their black colour and silvery luster in the field. These ore bodies are scattered in the form of irregular massive lenticular bodies with varying dimensions (see **Figure 3**). At places, the ores and host rocks (meta-cherts) contain cross-cutting fractures filled veins of quartz and carbonates. These ores and their host rocks are fragmented, folded, faulted and sheared suggesting that the metamorphism/deformation has occurred after the formation of these ores.

3. Methods

Detailed field work was carried out in the study area to collect representative samples from the Mn-ores and the host rocks, and also to identify the various field features, as shown in **Figure 3**. During fieldwork, 15 fresh looking samples of Mn-ores and 7 samples of host rocks (meta-chert) were collected for the experimental work in the Geochemistry Laboratory of the National Centre of Excellence in Geology (NCEG), University of Peshawar, Pakistan. These samples were crushed and pulverized to -200 mesh size, using a tungsten carbide cup mill (FRITSCH PULVERISETTE 9). The open-acid digestion technique after **Jeffery and Hutchison (1986)** using PTFE Teflon beakers was adopted whereby known weights of Mn-ores powdered samples were treated with HCL (10ml) and HF (5ml) for the complete digestion and known weights of host rock powdered samples were treated with HF: HNO3:HClO4 in the ratio of 7:3:1 for their complete digestion**.** The digested sample solutions of both ores and host rocks were analyzed for major oxides (i.e. MnO, Fe_2O_3, CaO, MgO, Na_2O and K_2O) and trace elements (i.e. Co, Cr, Cu, Cd, Pb, Ag and Ni) using Atomic Absorption Spectrometer (AAS) (**Perkin Elmer 7000**, equipped with graphite furnace) under the standard calibrated conditions. The analysis of SiO_2, TiO_2, P_2O_5, and Al_2O_3 was carried out using a Pye Unicam UV/visible spectrophotometer as described by **Jeffery and Hutchison (1986)**. The loss on ignition (LOI) was determined gravimetrically by heating the known weight of powdered samples of both ores and host rocks in a muffle furnace at 1200°C for four hours.

Petrographically, the Mn-ores and host rock samples were studied using polished thin sections under polarized and reflected light microscopy. For the identification of different Mn-bearing phases and gangue minerals X-ray diffraction (XRD: JEOL-JDX-3532) and scanning electron microscopic (SEM: JEOL-JSM-IT-100) techniques were carried out at the Centralized Resource Laboratory (CRL), and NCEG, University of Peshawar, respectively.

4. Results and Discussion

4.1. Petrography and Mineralogy

The XRD analysis of selected samples of the manganese ores revealed that two types of Mn-ore minerals, such as Mn silicate-oxide (braunite) and Mn-oxide (pyrolusite), are present in these ores along with quartz, calcite and hematite as accessory minerals (see **Figure 4**). Braunite, being the principal Mn-bearing phase, is in various shapes which range from microcrystalline to subhedral to euhedral coarse-grained. Microcrystalline braunite is intermixed with cryptocrystalline quartz, while the coarse-grained are interlocked having planar to sutured contacts, and the ore minerals are cross-cut by the quartz and calcite veinlets (see **Figure 5a**). Anhedral to subhedral, spindle and fibrous shaped pyrolusite grains are present in association with braunite and cryptocrystalline quartz (see **Figure 5b**). Pyrolusite also occurs as fractures filled phase (see **Figure 5a** and **e**). Cryptocrystalline quartz, a major accessory mineral, is generally enclosing the braunite, pyrolusite and piemontite (see **Figure 5b, f** and **d**). Piemontite and pyrolusite are replacing braunite at places (see **Figure 5e** and **g**). Fine-grained hematite is found in dissemination (see **Figure 5h**). In general, the coarse-grained quartz is found in the form of veins while the cryptocrystalline quartz is either enclosing or enclosed in the braunite (see **Figure 5h** and **i**). The petrographic features suggest that there could be two stages of formation of ore phases within the studied Mn-ores. The early stage is represented by massive braunite and minor pyrolusite minerals, while the late stage is characterized by replacement phases such as pyrolusite, piemontite and hematite. Braunite may have been altered to pyrolusite and hematite through chemical weathering and leaching due to silica removal and re-oxidation of Mn in low-grade surface environments (**Shaif et al. 2020; Safarov et al. 2024**) while the piemontite may have been formed by the alteration of braunite during medium to high-grade metamorphism (**Sinisi et al. 2018; Marescotti and Frezzotti 2000**).

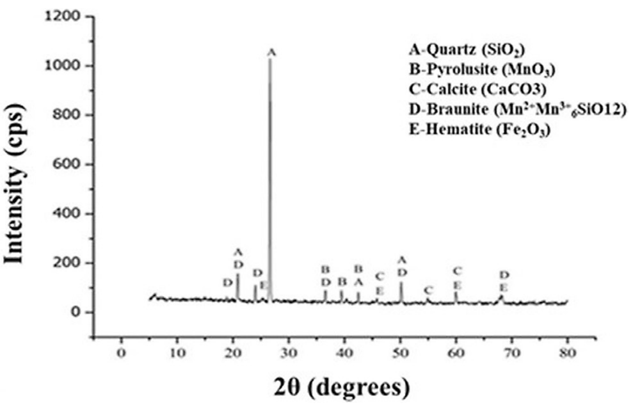

Figure 4. XRD graph showing the 2θ position of braunite, pyrolusite, hematite, quartz and calcite in the Mn-ores of the study area.

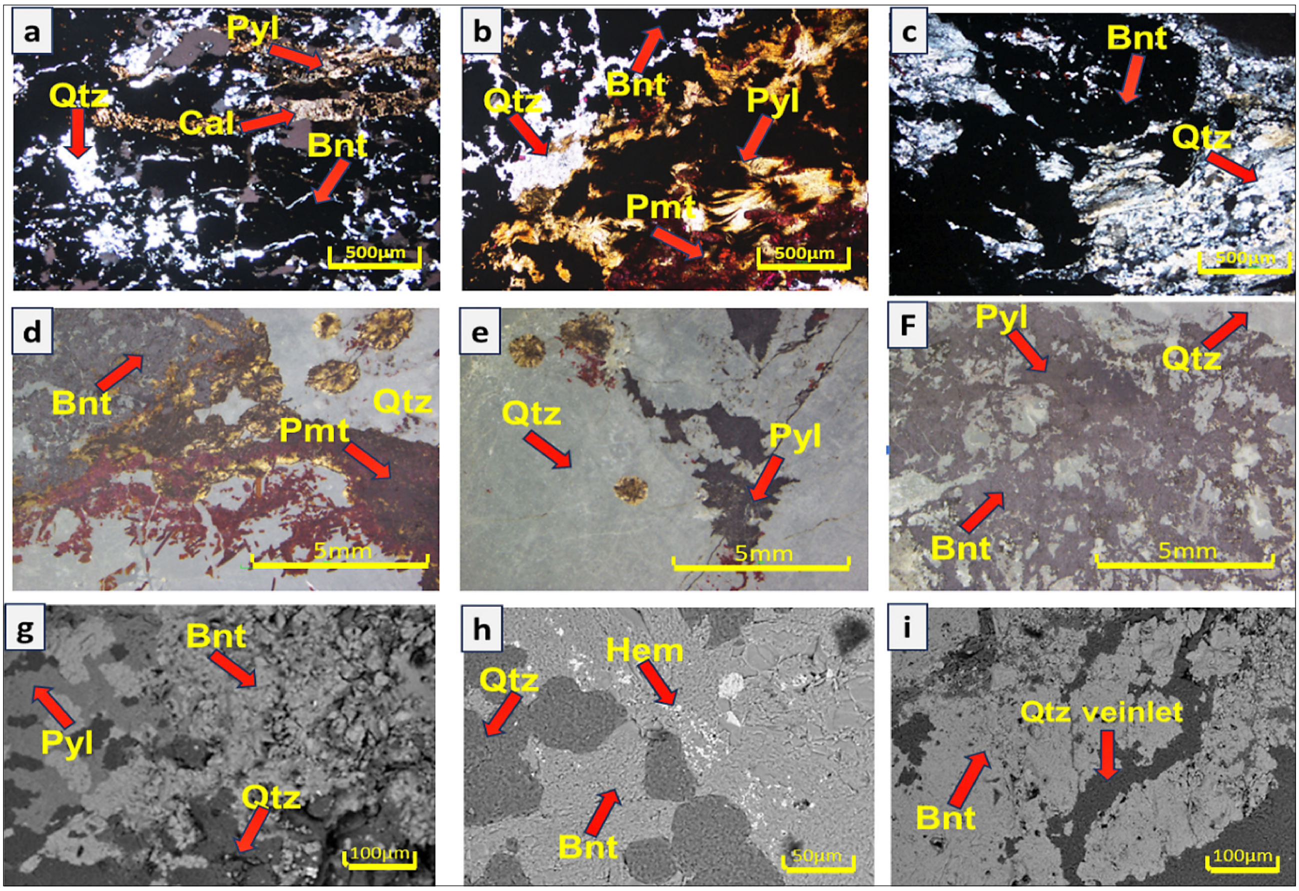

Figure 5. Photomicrographs (plane polarized: a-c; reflected light: d-f and SEM images: g-i) showing (a) veinlets of quartz and calcite cross-cutting the braunite grains while pyrolusite is present as fracture filled phase, (b) coarse-grained pyrolusite and piemontite are replacing braunite while spindle and fibrous shape pyrolusite is also visible (c) coarse-grained braunite is enclosed in cryptocrystalline quartz, (d) piemontite and braunite are enclosed in cryptocrystalline quartz, (e) pyrolusite occurs as fractured filled phase within cryptocrystalline quartz, (f) intermixing of braunite, pyrolusite and cryptocrystalline quartz, (g) pyrolusite is replacing braunite while quartz is also enclosed in braunite, (h) fine-grained hematite and quartz grains are present within braunite, (i) cryptocrystalline quartz veinlets are cross-cutting the Mn-minerals. **Abbreviation:** Bnt: braunite; Pyl: Pyrolusite; Qtz: Quartz; Hem: Hematite; Pmt: Piemontite; Cal: Calcite.

The meta-cherts, generally hosting the Mn-ores, are mainly composed of microcrystalline to cryptocrystalline quartz / chalcedony and a lesser amount of hematite. The pseudomorphs of radiolarian chert, occasionally replaced by microcrystalline quartz, hematite, carbonates and clay minerals, are also noticed.

4.2. Geochemistry

The representative samples of the studied Mn-ores and host rocks (i.e. meta-chert) have been analyzed for major and trace elements and the results are presented in the **Tables 1** and **2**, respectively. According to the classification of **Dorokhin et al. (1969)**, the studied Mn-ores, as of having 19.08 wt% to 45.21 wt% MnO, can be considered as low-grade (<35 wt% MnO), medium-grade (35-40 wt% MnO) and high grade (>40 wt% MnO) manganese ores. Economically, the studied Mn-ores, having 31.93 wt% MnO on average, can be termed as low-grade ores as a whole (see **Table 1**). The Mn-ores of the study area have SiO_2 contents ranging from 30.14 to 62.23 wt% (average: 48.41 wt%), TiO_2 from 0.03 to 0.46 wt% (average: 0.15 wt%), Al_2O_3 from 1.86 to 3.87 wt% (average: 2.68 wt%), Fe_2O_3 from 1.42 to 5.30 wt% (average: 3.26 wt%), MnO from 19.08 to 45.21 wt% (average: 31.93 wt%), MgO from 0.11 to 2.13 wt% (average: 0.91 wt%), CaO from 3.95 to 7.96 wt% (average: 5.85 wt%), Na_2O from 0.93 to 1.60 wt% (average: 1.22 wt%), K_2O from 0.02 to 1.30 wt% (average: 0.73 wt%) and P_2O_5 from 0.02 to 0.21 wt% (average: 0.08 wt%). Among the trace elements, Co is in the range of 2-48 ppm (average: 12 ppm), Cr: 1-56 ppm (average: 19 ppm), Cu: 8-402 ppm (average: 190), Cd: 1-5 ppm (average: 3 ppm), Pb: 10-131 ppm (average: 39 ppm), Ag: 1-17 ppm (average: 9 ppm) and Ni: 1-150 ppm (average: 65 ppm). All the trace elements are highly variable in the studied Mn-ores. The Mn/Fe and Fe/Mn ratios are also having greater variation and are ranging from 7.67 to 19.39 and 0.05 to 0.13 with the average values of 10.85 and 0.09, respectively. The major oxides have been corelated with the MnO in **Figure 6**. It has been found that all the major oxides, except SiO_2, exhibit no any correla-

Table 1. Geochemical analysis (major oxides in wt % and trace elements in ppm) in the Mn-ores of the Mohmand area.

Sample	IMS-1	IMS-2	IMS-3	IMS-4	IMS-5	IMS-6	IMS-7	IMS-8	IMS-9	IMS-10	IMS-11	IMS-12	IMS-13	IMS-14	IMS-15	MIN	MAX	AVG
SiO_2	48.61	42.53	38.21	41.45	30.14	36.15	38.25	57.21	62.23	55.61	52.45	56.01	55.28	54.02	57.96	30.14	62.23	48.41
TiO_2	0.03	0.08	0.24	0.03	0.11	0.16	0.08	0.34	0.09	0.20	0.05	0.09	0.06	0.46	0.23	0.03	0.46	0.15
Al_2O_3	2.65	2.22	2.06	2.14	3.02	1.86	3.87	2.18	3.06	3.23	2.98	3.23	3.23	2.55	1.99	1.86	3.87	2.68
Fe_2O_3	3.18	3.64	4.74	2.56	5.30	4.91	3.65	2.11	2.35	2.38	3.08	1.42	3.23	3.20	3.15	1.42	5.30	3.26
MnO	35.80	38.01	44.37	39.75	45.21	43.54	40.37	28.22	19.08	26.05	23.69	24.86	22.36	24.92	22.65	19.08	45.21	31.93
MgO	1.23	2.13	0.95	0.96	1.65	0.64	1.58	0.67	0.23	0.19	1.77	0.97	0.24	0.11	0.34	0.11	2.13	0.91
CaO	3.95	6.23	4.56	5.56	7.01	5.63	6.56	4.56	4.97	5.03	7.96	5.15	7.35	6.93	6.32	3.95	7.96	5.85
Na2O	0.93	1.00	1.16	1.38	1.07	1.60	1.09	1.60	1.31	1.11	1.17	1.30	1.24	1.10	1.23	0.93	1.60	1.22
K2O	0.80	1.10	0.71	0.06	0.24	1.10	1.30	0.02	1.23	0.03	1.14	0.98	0.88	0.44	0.85	0.02	1.30	0.73
P_2O_5	0.02	0.04	0.15	0.12	0.05	0.11	0.03	0.11	0.21	0.09	0.05	0.06	0.02	0.10	0.07	0.02	0.21	0.08
L.O.I	2.54	3.05	2.75	5.98	6.20	4.23	3.25	3.15	5.23	6.12	5.41	5.93	6.04	6.36	4.98	2.54	6.36	4.75
Total	99.73	100.10	99.89	99.87	100.20	99.93	100.00	100.10	99.99	99.98	99.75	100.01	99.92	100.19	99.78			99.96
Trace Elements																		
Co	10	48	28	25	22	10	4	2	3	2	2	3	3	7	5	2	48	12
Cr	17	56	33	23	25	9	17	4	1	7	5	12	7	14	52	1	56	19
Cu	210	229	402	74	325	345	185	97	8	168	209	189	153	129	122	8	402	190
Cd	3	2	5	1	3	2	2	3	3	3	2	2	4	3	2	1	5	3
Pb	19	131	95	20	75	21	28	19	34	10	21	38	26	23	31	10	131	39
Ag	1	4	1	4	11	8	12	12	12	11	17	10	12	12	9	1	17	9
Ni	26	35	123	98	125	98	52	1	18	34	19	50	19	150	131	1	150	65
Zn	30	25	20	50	10	121	60	14	18	40	35	42	29	65	35	10	121	39.6
Mn/Fe	12.47	11.56	10.37	17.19	9.45	9.82	12.25	14.81	8.99	12.12	8.52	19.39	7.67	8.62	7.96	7.67	19.39	10.84
Fe/Mn	0.08	0.09	0.10	0.06	0.11	0.10	0.08	0.07	0.11	0.08	0.12	0.05	0.13	0.12	0.13	0.05	0.13	0.09

MIN: Minimum; MAX: Maximum; AVG: Aver

Table 2. Geochemical analysis (major oxides in wt % and trace elements in ppm) of the host rocks (meta-cherts) of the Mohmand area.

Sample	HRS-1	HRS-2	HRS-3	HRS-4	HRS-5	HRS-6	HRS-7	MIN	MAX	AVG
SiO_2	80.13	81.25	81.11	79.56	82.65	78.23	79.56	78.23	82.65	80.36
TiO_2	0.03	0.15	0.041	0.056	0.011	0.21	0.096	0.01	0.21	0.08
Al_2O_3	4.52	6.25	4.69	7.54	4.95	8.41	5.11	4.52	8.41	5.92
Fe_2O_3	4.5	1.35	3.56	4.02	2.97	1.86	2.14	1.35	4.50	2.91
MnO	0.45	0.38	0.24	0.453	0.63	0.432	0.34	0.24	0.63	0.42
MgO	2.12	1.26	0.15	0.1	1.08	1.54	3.25	0.10	3.25	1.36
CaO	3.13	2.46	3.18	2.77	2.84	3.24	4.17	2.46	4.17	3.11
Na_2O	1.06	1.63	0.84	0.96	0.35	1.05	1.08	0.35	1.63	1.00
K_2O	0.76	0.98	0.85	0.65	0.92	1.63	1.14	0.65	1.63	0.99
P_2O_5	0.042	0.13	0.011	0.025	0.41	0.31	0.035	0.01	0.41	0.14
L.O.I	3.68	4.05	4.25	3.35	2.65	3.12	3.68	2.65	4.25	3.54
Total	100.42	99.88	98.92	99.48	99.46	100.03	100.60	98.92	100.60	99.83
Trace elements										
Co	7	8	7	11	5	12	8	5	12	8
Cr	8	6	3	114	13	8	11	3	114	23
Cu	26	103	49	53	5	44	71	5	103	50
Cd	3	4	3	4	3	3	2	2	4	3
Pb	17	15	10	7	16	12	9	7	17	12
Ag	7	7	4	6	1	6	7	1	7	5
Ni	17	70	9	28	10	52	49	9	70	33
Zn	56	60	49	66	80	41	47	41	80	57

tion with MnO. However, SiO_2 has well-defined positive correlation with MnO (see **Figure 6a**). This can be attributed to the formation of higher amount of braunite in the studied Mn-ores.

The studied meta-cherts are mainly composed of SiO_2 in the range of 78.23 to 82.65 wt%, Al_2O_3: 4.52 to 8.41 wt%, Fe_2O_3: 1.35 to 4.50 wt%, MgO: 0.10 to 3.25 wt% and CaO: 2.64 to 4.17 wt% while rest of the major oxides are in very low concentrations (see **Table 2**). The average concentration of trace elements such as Co, Cr, Cd, Pb, Ag and Ni in the studied mata-cherts are 8 ppm, 23 ppm, 50 ppm, 3 ppm, 12 ppm, 5 ppm and 33 ppm, respectively.

It is now well established that the geochemical characteristics of various types of manganese deposits have played a major role in characterizing the ancient analogues of hydrothermal and hydrogenous manganese deposits that are formed on the modern ocean floor (**Crerar et al. 1982**). During the precipitation of hydrothermal solution along the mid ocean ridges, the fractionation of Mn and Fe is resulted in the low and high Mn/Fe or Fe/Mn ratios in exhalative sediments (**Bonatti 1972; Bonatti et al. 1972, 1976; Shah and Khan 1999; Shah and Moon 2007; Khan et al. 2020**). The ratios of Mn/Fe are ranging from 7.67 to 19.39 and Fe/Mn from 0.05 to 0.13 in the studied Mn-ores. These ratios are consistent with that of the hydrothermal exhalative Mn-deposits formed in ophiolitic sequences and along the mid-ocean ridges (**Bonatti et al. 1972, 1976; Jach and Dudek 2005; Shah and Moon 2007; Jiancheng et al. 2013; Sasmaz et al. 2014**). Various researchers have used major and trace elements to distinguish manganese ores of hydrothermal and hydrogenous origin (**i.e. Bonatti et al. 1972; Toth 1980; Crerar et al. 1982; Adachi et al. 1986; Peters 1988; Choi and Hariya 1992; Nicholson 1992**). The geochemical data of the studied Mn-ores have been plotted in the discrimination diagrams, as shown in **Figure 7**. Almost all the samples fall within or close to the field of hydrothermal Mn-deposits in Co/Zn vs Co+Ni+Zn diagram (see **Figure 7a**) of **Toth (1980)**, Si vs Al diagram (see **Figure 7b**) of **Crerar eta al (1982)**, Zn-Ni-Co diagram (see **Figure 7c**) of **Choi and Harira (1992)** while in the Mn-Fe-(Ni+Co+Cu)*10 diagram (see **Figure 7d**) of **Bonatti (1972) and Crerar et al. (1982)**, the data fall in the overlapping fields of hydrothermal and diagenetic Mn-deposits.

The very low Fe/Mn ratio due to very low amount of Fe in the studied Mn-ores suggest that fractionation of Fe has occurred well before the formation of these ores (**Roy 1992; Frakes and Bolton 1992; Shah and Khan 1999; Shah and Moon 2007**). It is reported that the concentrations of trace elements (i.e. Cu, Zn, Ni and Co) in the modern submarine manganese deposits of East Pacific Rise and the Galapagos areas are higher than the pelagic sediments, but are much lower in the hydrother-

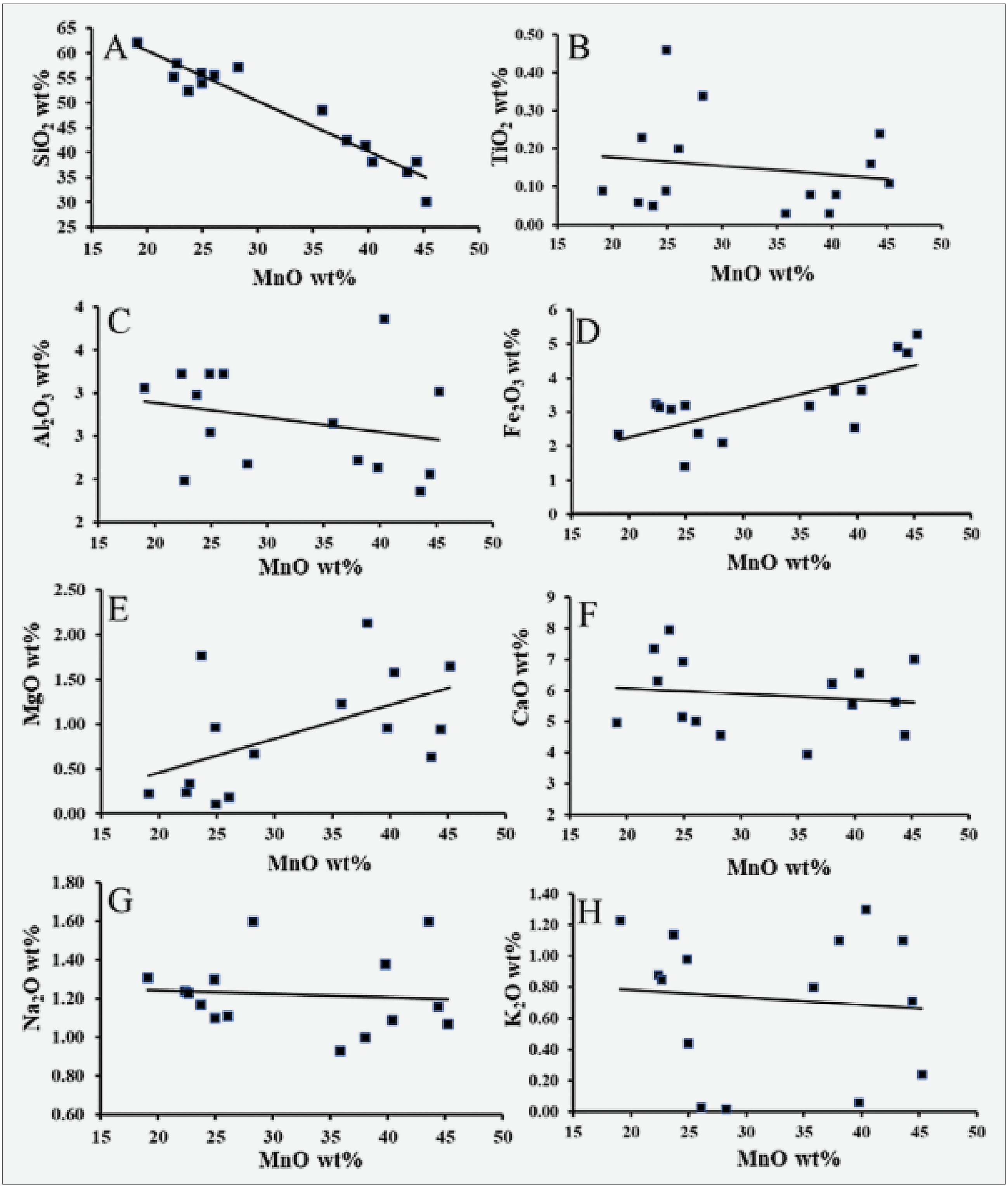

Figure 6. Major oxides versus MnO variation diagram of the studied Mn-ores.

mal Mn-deposits relative to the hydrogenous Mn-deposits (**Cronan 1980**). This is also confirmed in the case of the studied Mn-ores (see **Figure 7**). The plotting of the samples of studied Mn-ores along the Ni-Zn join line in **Figure 7c** also confirms the relationship of the studied Mn-ores with the modern submarine hydrothermal Mn-deposits. It is now well understood that the Fe compounds are less stable than the Mn compounds, whereby the Eh and/or pH is playing an important role, therefore, the precipitation of Fe has been reported proximal and Mn distal to the vent along the sea floor spreading centers (**Panagos and Varaavas 1984; Roy 1992; Frakes and Bolton 1992; Shah and Khan 1999; Shah and Moon 2004, 2007; Khan et al. 2010**).

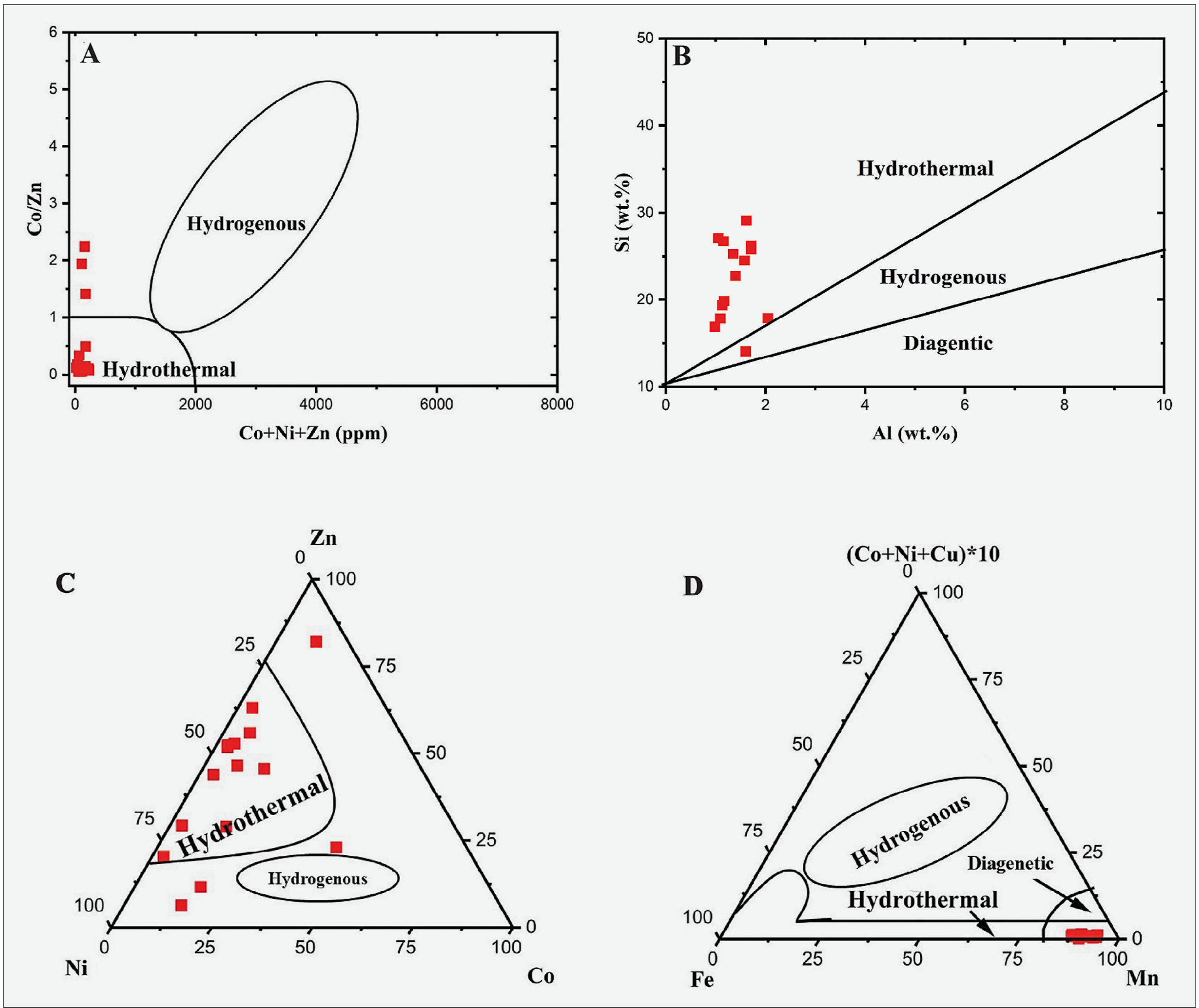

Figure 7. Plotting of the geochemical data of the studied Mn-ores from Mohmand area in the various discrimination diagrams: a) Co/Zn vs Co+Ni+Zn diagram of **Toth (1980)**; b) Al vs Si diagram of **Choi and Hariya (1992)**; c) Zn-Co-Ni diagram of **Choi and Hariya (1992)**; d) Mn-Fe-(Ni+Co+Cu) diagram of **Bonatti et al. (1972)** and **Crerar et al. (1982)**.

4.3. Genetic Model

The Nawagai ophiolitic melange in the Mohmand District, like the other ophiolitic melanges along MMT/ ISZ, are the remnants of the Neo-Tethys oceanic crust which were formed during the opening and closing of the Neo-Tethys with the later supra-subduction stage. These are later on obducted on to the Indian Plate during collision of the KIA with the Indian Plate in Late Cretaceous. The KIA was formed during the intra-oceanic subduction of the Neo-Tethys oceanic lithosphere and latter on merging with the Karakoram Plate to form an Andean type margin and finally collided with the Indian Plate (**Molnar and Tapponier 1975; Tahirkheli 1979; Klootwijk et al. 1992; Arif and Jan 2006; Ullah et al. 2025**).

By considering the models of **Bonatti et al. (1976), Canon and Force (1983), Buehn et al. (1992), Shah and Khan (1999), Khan et al. (2020), Ullah et al. (2025)**, a very simple genetic model can be proposed for the formation of the Mn-ores of the Mohmand area from the hydrothermal solution along the mid-ocean ridges in the Neo-Tethys and later on obduction of these ores within the Nawagai ophiolitic melange along MKT/ISZ (see **Figure 8**). According to this model, during the early stage (Late Jurassic) of Neo-Tethys Ocean, a mid-oceanic ridge setting was present where the sea water was percolating through the hot oceanic basaltic crust and resulted in the formation of hydrothermal solutions. During this process, the hydrothermal solutions started leaching out the Mn, Fe, Cu, Pb, Zn, Co, and other metals from the basaltic crust. These metals enriched hydrothermal solutions started discharging and precipitating on to the sea floor. Due to change in temperature and pressure and an increase in Eh and/or pH, the various metal sulfides started precipitating along or closer to the discharge vents, while the Fe and Mn fractionation in the form of ferromanganese and manganese ores took place

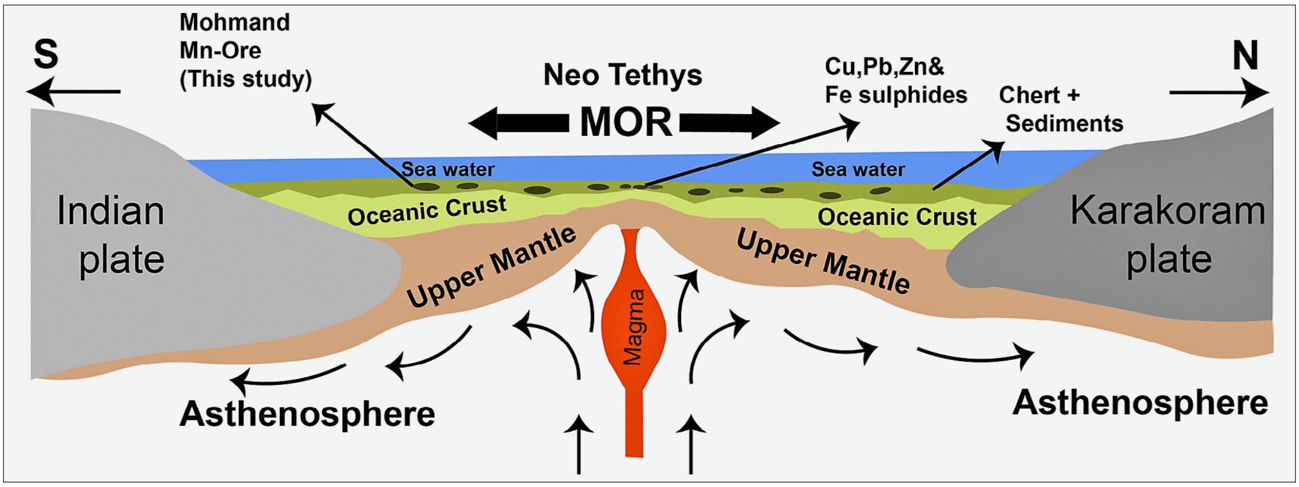

Figure 8. Hypothetical model showing the geological environment for the formation of Mohmand Mn-ores in the Neo-Tethys (modified after **Ullah et al. 2025**)

proximal and distal to the vent, respectively (**Bonatti et al. 1976; Crerar et al. 1982; Thornton and Seyfried 1985; Sawkins,1984; Roy 1992; Shanks et al. 1995; Shah and Khan 1999, Shah and Moon 2007; Khan et al. 2020**).

Considering the lower amount of Fe, higher amount of Si and higher Mn/Fe ratio in the Mn-deposits of the Mohmand area, these ores may have been formed distal to the discharge vent on the sea floor due to the early precipitation of ferromanganese ores near the source of hydrothermal solution and manganese ores distal to the source with input from the pelagic sediments within the mid-oceanic spreading center. This can be correlated with the present-day hydrothermal system within the mid-oceanic spreading centers (**Roy 1992; Shah and Khan 1999; Shah and Moon 2007; Narejo et al. 2019; Khan et al. 2020**). The development of mid-ocean ridges environment in the Neo-Tethys Ocean during Late Jurassic was followed by the origination of KIA by the northward double subduction during Early to Late Cretaceous. Afterwards, the closure of the Neo-Tethys Ocean and finally collision of KIA with the Indian Plate resulted in the formation of supra-subduction zone ophiolites, including the Nawagai ophiolitic melange, in northern Pakistan (**Ullah et al. 2025**).

The studied Mn-ores of the Mohmand area after their formation along the spreading centers were later on obducted on to the Indian Plate along the MMT/ISZ as part of the Nawagai ophiolitic melange during the subduction and later on collision of the Indian Plate with the Kohistan Island Arc. The field features such as the massive lenticular shape tectonized bodies with folding, faulting and shearing suggest that these ores and the host rocks may have undergone severe metamorphism and deformation during and after emplacement of the ophiolitic bodies in the existing position. This may have caused the recrystallization of manganese oxides and hydroxides into braunite by incorporating silica from the associated quartz (chert) during metamorphism. However, the essential geochemical characteristics of the deposits remained intact (see also **Bonatti et al. 1976; Shah and Khan 1999; Khan et al. 2020**). The geochemical characteristics of the studied Mn-ore bodies of the Mohmand area occurring in the Nawagai ophiolitic melange have been compared with the hydrothermal manganese deposits of other ophiolitic sequences elsewhere in the world in **Table 3**, for example, the Bela ophiolitic complex, Pakistan (**Narejo et al. 2019**); the Zhob ophiolites, Pakistan (**Khan et al. 2020**), the Waziristan ophiolite complex, Pakistan (**Shah and Khan 1999; Shah and Moon 2007**), Dehoo, ophiolitic unit, Iran (**Lotfi et al. 2017**), Cayirli, Ankara ophiolitic melange, Turkey (**Zarasvandi et al. 2013**) and Wakasas, Tokoro Belt, Hokkaido, Japan (**Öksüz 2011**). The studied Mn-ores of Mohmand area are very well correlated with the hydrothermal manganese deposits associated with ophiolitic sequences elsewhere in the world by having a higher Mn/Fe ratio, lower Fe/Mn ratio and lesser amount of trace elements (**Table 3**) as compared to hydogenous manganese deposits (**Nicholson et al, 1997; Jach and Dudek 2005**).

5. Conclusions

Manganese ores of the district Mohmand occur in the form of lenticular and irregular bodies of varying dimensions with cross-cutting quartz veins associated with cryptocrystalline meta-chert in the Nawagi ophiolitic melange zone. The ore bodies are highly sheared and fractured and these fractures are filled in by quartz and carbonates in the form of veins. Braunite is the dominant Mn-bearing phase with a lesser amount of pyrolusite and piemontite. Microcrystalline quartz, calcite and hematite occur as gangue minerals. Geochemical data suggest that the major and trace elements are highly variable in these ores and on the basis of the presence of Mn and Fe contents, these ores can be classified as high to low-grade but economically, as a whole, these ores can be considered as low-grade. The geochemical data further suggest that these ores have been formed due to the precipitation of hydrothermal solution distal to the discharge source (vent) with some input from the pelagic sediments on the sea floor within the spreading centers in the Neo-Tethys Ocean during Late Jurassic. These ores are then obducted on to the Indian Plate as part of the Nawagai ophiolitic melange due to the subduction and later on collision of Indian Plate with the KIA along the MMT/ISZ during Late Cretaceous.

Acknowledgement

We are very thankful to the Director, National Centre of Excellence in Geology, University of Peshawar for providing financial support for field work and laboratory work to the first author for his MS research. The Director Centralized Resource Laboratory, University of Peshawar is thanked for the X-ray Diffraction analysis. Mr. Muhammad Tariq, Lab Technician, and Mr. Uzair Ahmad, Lab Technician, are also thanked for their assistance during the geochemical and SEM analyses, respectively.

6. References

Adachi M, Yamamoto K, Sugisaki R (1986). Hydrothermal chert and associated siliceous rocks from the modern Pacific: their geologic significance as indication of ocean ridge activity. Sedimentary Geology, 47: 125±148.

Ahmad I, Jehan N (2006). Occurrence of a melange along the Malakand pass north of Dargai, northern Pakistan. *Journal of Himalayan Earth Science,* 39: 55-59.

Arif M, Jan MQ (2006). Petrotectonic significance of the chemistry of chromite in the ultramafic-mafic complexes of Pakistan. *Journal of Asian Earth Sciences,* 27: 628–646. https://doi.org/10.1016/j.jseaes.2005.06.004.

Aslam, M., Hussain, A., Ashraf, M., Afridi, A.G.K., 2006. Geological Map of North West Frontier Province Pakistan, first ed. Directorate of publication geological survey of Pakistan Quetta: Quetta.

Baba AA, Ibrahim L, Adekola FA, Bale RB, Ghosh MK, Sheik AR, Pradhan, BS, Treloar P (2003) Northward subduction of the Indian Plate beneath the Kohistan island arc, Pakistan Himalaya: new evidence from isotopic data. *Jornal of Geological Society* 160(3): 377-384.

Bard JP (1983). Metamorphism of an obducted island arc: Example of the Kohistan sequence (Pakistan)in the Himalayan Collided range. *Earth and Planetary Science Letters,* 65: 133-144.

Bonatti E, Kraemer T, Rdell H (1972). Classification and genesis of submarine iron-manganese deposits. In: Horn D (ed) Ferro-manganese deposits on the ocean: International Decadron Ocean Exploration Washington DC Nation Sci Found 149±166.

Bonatti E, Zerbi M, Kay R, Rydell H (1976). Metalliferous deposits from the Apennine ophiolites: Mesozoic equivalents of modern deposits from oceanic spreading centers. *Geological Society of American Bulletin,* 87:83±94.

Bonatti E (1972). Classification and genesis of submarine iron-manganese deposits.

Buehn B, Stanistreet IG, Okrusch M (1992). Late Proterozoic outer shelf manganese and iron deposits at Otjosondu (Namibia) related to the Damaran oceanic opening. *Economic Geology,* 87: 1393±144.

Burg JP, Chaudhry MN, Ghazanfer M, Anczkiewicz R, Spencer D (1996). Structural evidence of back sliding of Kohistan arc in the collision system of the northwest Pakistan. *Geology,* 24: 739-742.

Cannon WF, Force ER (1983). Potential for high-grade shallow-marine manganese deposits in North America. In: Shanks WCIII (ed) Cameron volume on unconventional mineral deposits. New York Society Mining Engineers/ American Institute of Mining, *Metallurgy and Petroleum Engineers,* 177±190.

Choi JH, Hariya Y (1992). Geochemistry and depositional environment of Mn oxide deposits in the Tokoro Belt, northeastern Hokkaido, Japan. *Economic Geology*, 87(5): 1265-1274.

Choukrad J, Ouahzizi Y, Ali AA, Charroud M (2022). Geology, mineralogy, geochemistry and deposit model of iron and manganese in Bouarfa mine, Eastern High Atlas Morocco. *Scientific African,*18:e01401. https://doi.org/10.1016/j.sciaf.2022.e01401

Chyi MS, Crerar DA, Carlson RW, Stallard RF (1984). Hydrothermal Mn-deposits of the Francisean assemblage, II. Isotope and trace element geochemistry, and implication for hydrothermal convection at spreading centres. *Earth and Planetary Science Letters,* 71: 31±45

Crerar DA, Namson J, Chyi MS, Williams L, Feigenson MD (1982). Manganiferous cherts of the Franciscan assemblage; I, General geology, ancient and modern analogues, and implications for hydrothermal convection at oceanic spreading centers. *Economic Geology*, 77(3): 519-540.

Cronan DS (1980) Underwater minerals: Academic Press, Lond, 362p

DiPietro JA, Ahmad I, Hussain A (2008). Cenozoic kinematic history of the Kohistan fault in the Pakistan Himalaya. *Geological Society of American Bulletin,* 120(11-12): 1428-1440.

DiPietro JA, Hussain A, Ahmad I, Khan MA (2000). The Main Mantle Thrust in Pakistan: its character and extent. *Geological Society of London Special Publication,* 170(1): 375-393.

DiPietro JA, Pogue R (2004). Tectonostratigraphic subdivisions of the Himalaya: A view from the west. *Tectonics*, 23(5), 1-20. TC5001, doi:10.1029/2003TC001554.

DiPietro, J. A. (1991), Metamorphic pressure-temperature conditions of Indian plate rocks south of the Main Mantle Thrust, Lower Swat, Pakistan, Tectonics, 10, 742–757

Dorokhin IV, Bogachero EN, Druzhiniv AV, SoboleviskiVI, Gorbunov EV (1969). Economic mineral deposits. *Higher School, Moscow*, 368.

Fleet A, Robertson AHF (1980). Ocean-ridge metalliferous and pelagic sediments of the Semail Nappe, Oman. *Journal of the Geological Society of London* 137: 403±422

Frakes L, Bolton BR (1992). Effects of Ocean Chemistry, Sea Level, and Climate on the Formation of Primary Sedimentary Manganese *Ore Deposits. Economic Geology*, 87(5): 1207–1217. https://doi.org/10.2113/gsecongeo.87.5.1207

Haider SK, Azimi G, Duan L, Anthony EJ, Patchigolla K, Oakey JE, Leion H, Mattisson T, Lyngfelt A (2016). Enhancing properties of iron and manganese ores as oxygen carriers for chemical looping processes by dry impregnation. *Applied Energy,* 163: 41-50.

Hein JR, Gibbs AE, Clague DA, (1996). Hydrothermal mineralization thermal convection at spreading centres. *Earth and Planetary Science Letters,*71: 31±45

Hein JR, Koschinsky A, Halbach P (1997). Iron and Manganese Oxide Mineralization in the Pacific. In: Nicholson K, Hein JR, Buhn B (eds) Manganese Mineralization: Geochemistry and Mineralogy of Terrestrial and Marine Deposits. *Geological Society Special Publication,* 123–138.

Hein JR, Mizell K, Koschinsky A, Conrad TA (2013). Deep-ocean mineral deposits as a source of critical metals for high- and greentechnology applications: comparison with land-based resources. *Ore Geology Reviews,* 51:1–14. https://doi.org/10.1016/j.oregeorev.2012. 12.001

Ingram BL, Hein JR, Farmer GL (1990). Age Determinations and Growth Rates of Pacific Ferromanganese Deposits Using Strontium Isotopes. *Geochimica et Cosmochimica Acta,* 54(6): 1709–1721. https://doi.org/10.1016/0016-7037(90)90402-7

Jach R, Dudek T (2005). Origin of a Toarcian manganese carbonate/silicate deposit from the Krížna unit, Tatra Mountains, Poland. *Chemical Geology*,224(1-3): 136-152.

Jeffery PG, Hutchison D (1986). Chemical methods of rock analysis. *Prgamon Press, New York*, 370p.

Jiancheng X, Weidong S, Jianguo D (2013) Geochemical studies on Permian manganese deposits in Guichi, eastern China. Implications for their origin and formative environments, *Journal of Asian Earth Sciences,* 74: 155–166.

Karakuş A, Yavuz B, Koç S (2010). Mineralogy and Major-Trace Element Geochemistry of the Haymana Manganese Mineralizations, Ankara, Turkey. *Geochemistry International*, 48(10): 1014–1027. https://doi.org/10.1134/s00167 0291010006x.

Kazmi, A. H., R. D. Lawrence, H. Dawood, L. W. Snee, and S. Hussain (1984), Geology of the Indus suture zone in the Mingora-Shangla area of Swat, N. Pakistan, Geological Bulliten University of Peshawar,, 17, 127–144

Kazmi A, Jan M (1997). Geology and Tectonics of Pakistan Graphic Publishers.

Khan MA (ed), Aslam M, Hussain A, Ashraf M, Afridi AGK (Authors) (2006). Geological map of North West Frontier Province, Pakistan (Colored, Scale 1:1,000,000). *Geological Survey of Pakistan* (Map Series).

Khan MA, Jan MQ, Weaver BL (1993). Evolution of the lower arc crust in Kohistan, N. Pakistan: temporal arc magmatism through early, mature and intra-arc rift stage. In: Treloar PJ and Searl MP (eds) Himalayan Tectonics. *Geological Society of London Special Publications,* 74: 123-138.

Khan MA, Kakar MI, Ulrich T, Ali L, Kerr AC, Mehmood K, Siddiqui RH (2020). Genesis of Manganese Deposits in the Ali Khanzai Block of the Zhob Ophiolite, Pakistan: Inferences from Geochemistry and Mineralogy. *Journal of Earth Sciences* 31(5) 884–895.

Klootwijk CT, Gee JS, Peirce JW, Smith GM, McFadden PL (1992). An early India- Asia contact: paleomagnetic constraints from Ninety east ridge, ODP Leg 121. *Geology* 20(5): 395-398.

Kuhn T., Bau M, Blum, N, Halbach P (1998). Origin of Negative Ce Anomalies in Mixed Hydrothermal-Hydrogenetic Fe-Mn Crusts from the CentralIndian Ridge. 163(1/2/3/4): 207–220. https://doi.org/10.1016/s0012-821x(98)00188-5.

Lasheen TA, El-Hazek MN, Helal AS El-Nagar W (2009). Recovery of Manganese Using Molasses as Reductant in Nitric Acid Solution. *International Journal of Mineral Processing*, 92: 109-114. https://doi.org/10.1016/j.minpro.2009.03.001

Lee JS (1982). Manganese deposits and plate tectonics, Olympic Peninsula, Washington. Abstr I.A.G.O.D. 6th, *Symposium of Tbilisi*, 6±12, 295±296.

Lotfi M, Kahrazehi M, Ghaderi M (2017). Geochemistry and Origin of Dehoo Manganese Deposit, South Zahedan, Southeastern Iran. *Arabian Journal of Geosciences*, 10(6): 142. https://doi.org/10.1007/s12517-017-2865-8.

Marescotti P, Frezzotti M (2000). Alteration of braunite ores from Eastern Liguria (Italy) during syntectonic veining processes: Mineralogy and fluid inclusions. *European Journal of Mineralogy,* 12(2):341-356.

Mehdilo A, Irannajad M (2014). Evaluation of pyrolusite flotation behavior using a cationic collector. *Journal of Mining Science,* 50(5): 982-993.

Molnar P, Tapponnier P, (1975). Cenozoic tectonics of Asia: effects of a continental collision. *Science* 189: 419-426

Narejo AA, Shar AM, Fatima N, Sohail K (2019). Geochemistry and origin of Mn deposits in the Bela ophiolite complex, Balochistan, Pakistan. *Journal of Petroleum Exploration and Production Technology,* 9:2543–2554

Naseem S, Sheikh SA, Mallick KA (1997) Lithiophorite and associated manganese mineralization in Lasbela area, Balochistan, Pakistan. *Geosciences Journal* 1(1): 10-15.

Nicholson K (1992). Contrasting mineralogical-geochemical signatures of manganese oxides; guides to metallogenesis. *Economic Geology* 87(5): 1253-1264.

Nicholson K, Nayak VK., Nanda JK (1997). Manganese Ores of the Ghoriajhor-Monmunda Area, Sundergarh District, Orissa, India: Geochemical Evidence for a Mixed Mn Source. *Geological Society* of *London Special Publication,* 119(1): 117–121. https://doi.org/10.1144/gsl.sp.1997. 119.01.08.

Öksüz N (2011). Geochemical characteristics of the Eymir (Sorgun-Yozgat) manganese deposit, Turkey. *Journal of Rare Earths,* 29(3): 287–296

Öksüz N, Okuyucu N (2014). Mineralogy, geochemistry, and origin of Buyukmahal manganese mineralization in the Artova ophiolitic complex, Yozgat, Turkey. *Journal of Chemistry,* 2014:837972. https ://doi.org/10.1155/2014/ 83797 2

Panagos AG Varanavas SP (1984). On the genesis of some manganese deposits from eastern Greece, Syngenesis and Epigenesis in the Formation of Mineral Deposits 553–561.

Polgári PMO (1991). Stable Isotope Evidence for the Origin of the Urkut Manganese Ore Deposit, Hungary. *J Sed Res* 61(3): 384–393. https://doi.org/10.1306/d426771c-2b26-11d7-8648000102c1865d

Polgári M, Hein J, Vigh T, Szabó-Drubina M, Fórizs I, Bíró L, Müller A, Tóth A (2012). Microbial processes and the origin of the Úrkút manganese deposit, Hungary. *Ore Geology Reviews* 47: 87-109.

Rehman WU, Rehman AU, Khan F, Muhammad A, Younas M (2020). Studies on beneficiation of manganese ore through high intensity magnetic separator. *Advanced Science and Engineering*,12(1): 21-27.

Robertson A (2000). Formation of melanges in the Indus suture zone, Ladakh Himalaya by successive subduction-related, collisional and post-collisional processes during late Mesozoic-late Tertiary time. *Geological Society of London Special Publications,* 170(1): 333-374.

Roy S (1992). Environments and processes of manganese deposition. *Economic Geology* 87(5) 1218–1236.

Safarov RZ, Kargin JB, Zhandildenova AK, Aibuldinov YK, Vatin NI, Seo J, Barnes CHW, Valladares LDLS (2024) Oxide Metamorphic Manganese Ores: An Experimental Results of Heat Treatment. *Preprints.org.* 1-15.

Sasmaz A, Turkyilmaz B, Ozturk N (2014). Geology and geochemistry of middle Eocene madden complex ferromanganese deposits from Elazı˘g-Malatya Region, Eastern, Turkey. *Ore Geology Reveiws* 56: 352–372.

Sawkins FJ (1984). Metal deposits in relation to plate tectonics. 2nd Ed. *Springer-Vereng, Berlin*.

Searle M, Khan MA, Fraser J, Gough S, Jan MQ (1999). The tectonic evolution of the Kohistan- Karakoram collision belt along the Karakoram Highway transect, north Pakistan. *Tectonics* 18(6): 929-949.

Shah MT, Moon CJ (2004). Mineralogy, geochemistry and genesis of the ferromanganese ores from Hazara area, NW Himalayas, northern Pakistan. *Journal Asian Earth Sciences,* 23(1): 1-15.

Shah M, Khan A, (1999). Geochemistry and origin of Mn-deposits in the Waziristan ophiolite complex, north Waziristan, Pakistan. *Mineralium Deposita,* 34(7): 697-704.

Shah MT, Moon CJ, (2007). Manganese and ferromanganese ores from different tectonic settings in the NW Himalayas, Pakistan. *Journal Asian Earth Sciences* 29, 455-465.

Shaif M, Siddiquie FN, Ahmad M (2020). Mineralogical Studies of the Manganese Ores in Banswara Manganese Belt, Banswara District, Rajasthan Available to Purchase *Journal of Geological Society of India,* 96 (2): 189–198.

Shanks WC, Bohlke JK, Seal RR (1995). Stable isotopes in mid-ocean ridge hydrothermal system: implications between fluid, mineral and organism. *Geophysical Monograph Ser,*194-221.

Siddiquie F, Burhamuddin K, Shaif, M, Alam S (2015). Manganese ore minerals assemblages and mineral paragenesis with the help of ore petrography and XRD studies of Balaghat District,(MP) India. *Global Journal of Science Frontier Research: Environment & Earth Science,* 15(3): 21-34.

Sinisi R, Mongelli G, Peri F, Rizzo G (2018). The braunite (3Mn2O3·MnSiO3)-rich mineralization in the metasedimentary succession from southern Apennines (Italy): Genesis constraints. *Ore Geology Reveiws*, 94(169), 1-11. https://doi.org/10.1016/j.oregeorev.2018.01.014

Tahirkheli RK (1979). Geology of Kohistan and adjoining Eurasian and Indo-Pakistan continents, Pakistan. *Geological Bulliten University of Peshawar*, 11(1): 1-30.

Tahirkheli RK (1979). The India-Eurasia suture zone in northern Pakistan: Synthesis and interpretation of recent data at plate scale. *Geodynamics of Pakistan* 125-130.

Thornton EC, Seyfried Jr WE (1985). Sediment–sea water interaction at 200_and 300 C, 500 bars pressure: the role of sediment composition in diagenesis and lowgrade metamorphism of marine clay. *Geological Society of America Bulletin*, 96: 1287–1295.

Toth JR (1980). Deposition of submarine crusts rich in manganese and iron. *Geol Soc Amer Bull* 91(1): 44-54.

Treloar PJ (1989). Imbrication and unroofing of the Himalayan Thrust stack of the north Indian plate, north Pakistan. *Geological Bulletin University of Peshawar* 22: 25-44.

Ullah Z, Khan A, Li H, Zafat T, Ali A, Farhan M, Hussain Z, Khan A, Idress M, Ibrar M (2025). Petrogenesis and tectonic implications of peridotites of the Shangla Complex Ophiolite along Main Mantle Thrust, Northern Pakistan. Geoscience Frontiers. Published online 2025:102070.

Usui A, Nishimura A (1992). Submersible Observations of Hydrothermal Manganese Deposits on the Kaikata Seamount, Izu-Ogasawara (Bonin) Arc. *Marine Geology*, 106(3/4): 203–216. https://doi.org/10.1016/0025-3227(92)90130-a

Usui A, Someya M (1997). Distribution and Composition of Marine Hydrogenetic and Hydrothermal Manganese Deposits in the Northwest Pacific. *Geological Society London Special Publication* 119(1): 177–198. https://doi.org/10.1144/gsl.sp.1997.119.01.12

SAŽETAK

Geokemija i geneza manganovih ruda u ofiolitnome melanžu Nawagai, okrug Mohmand, Khyber Pakhtunkhwa, Pakistan

Ofiolitni melanž Nawagai nalazi se u zapadnome dijelu glavne navlake plašta Indske suturne zone (MMT/ISZ) u sjevernome Pakistanu i smatra se dijelom naboranoga pojasa koji sadržava ofiolitne sekvencije. Istraživana tijela manganove rude prisutna su u ofiolitnome melanžu Nawagai u okrugu Mohmand u Khyber Pakhtunkhwi u Pakistanu. Ove rude dislocirana su lećasta tijela različitih veličina i općenito su povezana s kriptokristalastim metarožnjakom. Manganove rude i metarožnjaci jako su tektonizirani te su podložni metamorfizmu/deformaciji. Mineraloški, istraživane manganove rude dominantno se sastoje od braunita s manjom količinom piroluzita i piemontita kao faza koje sadržavaju Mn, dok se minerali jalovine uglavnom odnose na kriptokristalasti kvarc s manjom količinom kalcita. Manganove faze isprepletene su unutar kriptokristalastoga kvarca; međutim uočavaju se i poprečne mikrožile kvarca i kalcita. Na pojedinim mjestima piroluzit i piemontit zamjenjuju braunit. Geokemijski istraživane manganove rude vrlo su varijabilne po svojemu sadržaju. Općenito su od visokoga do niskoga sadržaja, no u cijelosti, s ekonomskog gledišta mogu se smatrati rudama niskoga obogaćenja gledajući sadržaj MnO, Fe_2O_3 i SiO_2. Nije pronađena korelacija među glavnim elementima, međutim uočena je znatna pozitivna korelacija između SiO_2 i MnO. Frakcioniranje Mn i Fe te koncentracije različitih glavnih i elemenata u tragovima upućuju na to da su proučavane manganove rude područja Mohmand nastale iz hidrotermalnoga fluida distalno od izvora (hidrotermalnoga izvora) uz doprinos iz pelagičnih sedimenata duž srednjooceanskih grebena unutar Neotetisa. One su prenesene kao egzotična tijela unutar ofiolitskih sekvencija na Indijsku ploču uslijed subdukcije Indijske ploče ispod otočnoga luka Kohistan duž MMT/ISZ. Ove manganove rude i metarožnjaci pretrpjeli su jak metamorfizam i deformaciju tijekom i nakon postavljanja ofiolitskih tijela u postojeći položaj.

Ključne riječi:
mangan, petrografija, mineralogija, geokemija, geneza rude

Author's contribution

Irfan Ullah (MS Scholar): conceptualization, methodology, field investigation, data curation, and draft writing **Aamir Khan** (PhD Scholar): contributed to data curation, conceptualization, reviewing, editing, and writing the original draft. **Muhammad Tahir Shah** (PhD, Professor) contributed to conceptualization, complilation, reviewing and editing. **Liaqat Ali** (PhD, Professor): supervision, data curation, reviewing and editing and funding acquisition. **Asad Khan** (PhD, lecturer) contributed to laboratory work, and data support.
All authors have read and agreed to the published version of the manuscript.